ARTICLES
https://doi.org/10.1038/s41559-019-0954-7

nature ecology & evolution

Corrected: Author Correction

Continental scale structuring of forest and soil diversity via functional traits

Vanessa Buzzard[1*], Sean T. Michaletz[1,2,3], Ye Deng[4,5], Zhili He[4,6,7], Daliang Ning[4], Lina Shen[4], Qichao Tu[4,8], Joy D. Van Nostrand[4], James W. Voordeckers[4], Jianjun Wang[4], Michael D. Weiser[9], Michael Kaspari[9,10], Robert B. Waide[11], Jizhong Zhou[4,12,13] and Brian J. Enquist[1,14]

Trait-based ecology claims to offer a mechanistic approach for explaining the drivers that structure biological diversity and predicting the responses of species, trophic interactions and ecosystems to environmental change. However, support for this claim is lacking across broad taxonomic groups. A framework for defining ecosystem processes in terms of the functional traits of their constituent taxa across large spatial scales is needed. Here, we provide a comprehensive assessment of the linkages between climate, plant traits and soil microbial traits at many sites spanning a broad latitudinal temperature gradient from tropical to subalpine forests. Our results show that temperature drives coordinated shifts in most plant and soil bacterial traits but these relationships are not observed for most fungal traits. Shifts in plant traits are mechanistically associated with soil bacterial functional traits related to carbon (C), nitrogen (N) and phosphorus (P) cycling, indicating that microbial processes are tightly linked to variation in plant traits that influence rates of ecosystem decomposition and nutrient cycling. Our results are consistent with hypotheses that diversity gradients reflect shifts in phenotypic optima signifying local temperature adaptation mediated by soil nutrient availability and metabolism. They underscore the importance of temperature in structuring the functional diversity of plants and soil microbes in forest ecosystems and how this is coupled to biogeochemical processes via functional traits.

A key challenge in developing a predictive framework for ecosystem functioning is that we lack a mechanistic understanding of the relationships between climate, plant traits, microbial traits and ecosystem processes[1,2]. While analyses of community trait compositions are increasingly used to understand the processes shaping biodiversity and biogeography, the links between above-ground traits and below-ground microbial processes remain largely unknown[3,4]. Nonetheless, an implicit assumption in trait-based ecology is that generalizable relationships between traits and the environment are linked across trophic levels to influence ecosystem processes[5,6]. Although recent studies have developed conceptual frameworks for understanding the distribution of traits in diverse trophic groups[7–11], most empirical research has focused on plant traits[5,12–15] (but see refs. [16,17]) and few studies have directly examined relationships between traits across many trophic groups using locally collected data[1,18–21].

Here, we provide a conceptual framework for understanding how traits vary along a temperature gradient if both plants and microbes are independently driven by the same thermodynamics (Fig. 1). Building on past studies, Fig. 1 uses the life history/resource acquisitive-conservation continuum[22] to graphically organize predictions from several trait-based hypotheses along a temperature gradient. A finding of macroecology and biogeography is that temperature is a central driver that shapes and shifts variation in biological diversity[23] (Fig. 1). Furthermore, trait-based ecology has shown that temperature is a central driver of plant diversity via selection on traits linked to plant hydraulics, leaf energy balance, carbon and water gas exchange and nutrient use[22,24]. Trait-based ecology states that such environmentally driven variation and shifts in traits will in turn influence ecosystem functioning (Fig. 1)[2]. Indeed, shifts in the distribution and diversity of plant functional traits have been linked to variation in rates of nutrient uptake[25], litter decomposition[25,26] and ecosystem productivity[27]. Also, it has been shown that plant traits related to the resource acquisition-conservation continuum may scale up to influence ecosystem-level nutrient cycling[6,28–30]. Since microbes play a critical role in the regulation of ecosystem functioning via decomposition and nutrient cycling, an emergent prediction of trait-based ecology is that shifts in temperature should be associated with corresponding shifts in plant traits and microbial function, resulting in ecological feedbacks between plants and microbes[31–33].

In Fig. 1, we can use the resource acquisition-conservation continuum and the above findings to make predictions for shifts in plant traits across temperature gradients and assess how these

[1]Department of Ecology and Evolutionary Biology, University of Arizona, Tucson, AZ, USA. [2]Los Alamos National Laboratory, Earth and Environmental Sciences Division, Los Alamos, NM, USA. [3]Department of Botany and Biodiversity Research Centre, University of British Columbia, Vancouver, British Columbia, Canada. [4]Institute for Environmental Genomics and Department of Microbiology and Plant Biology, School of Civil Engineering and Environmental Sciences, University of Oklahoma, Norman, OK, USA. [5]Chinese Academy of Sciences, Key Laboratory of Environmental Biotechnology, Research Center for Eco-Environmental Sciences, Beijing, China. [6]Environmental Microbiomics Research Center, School of Environmental Science and Engineering, Sun Yat-sen University, Guangzhou, China. [7]Southern Marine Science and Engineering Guangdong Laboratory, Zhuhai, China. [8]Institute of Marine Science and Technology, Shandong University, Qingdao, China. [9]Geographical Ecology Group, Department of Biology, University of Oklahoma, Norman, OK, USA. [10]Smithsonian Tropical Research Institute, Balboa, Republic of Panama. [11]Department of Biology, University of New Mexico, Albuquerque, NM, USA. [12]Earth and Environmental Sciences, Lawrence Berkeley National Laboratory, Berkeley, CA, USA. [13]State Key Joint Laboratory of Environment Simulation and Pollution Control, School of Environment, Tsinghua University, Beijing, China. [14]The Santa Fe Institute, Santa Fe, NM, USA. *e-mail: vbuzzard@email.arizona.edu

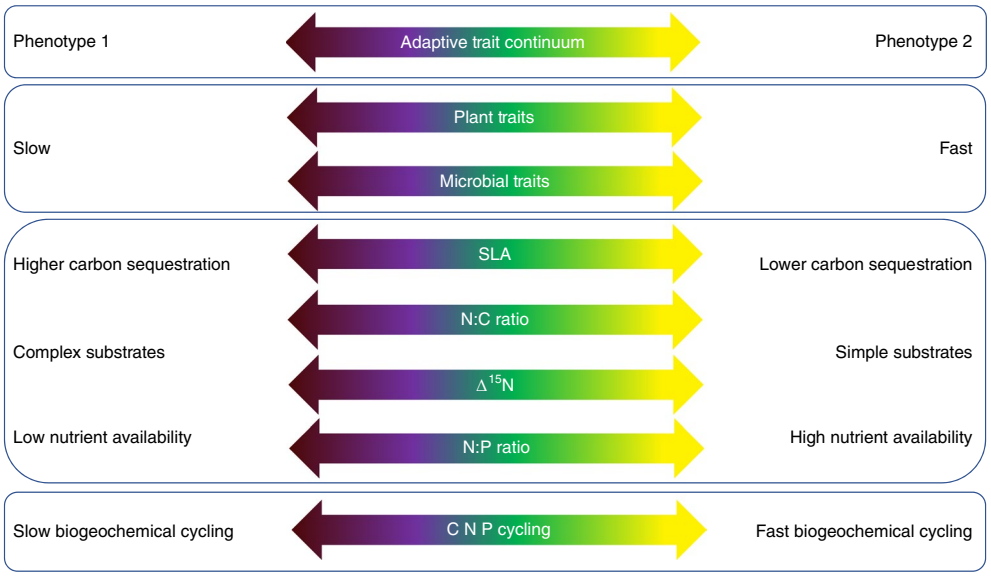

Fig. 1 | Coordinated trade-offs in plant functional traits and their relation to microbial and ecosystem processes. Temperature is a primary environmental driver that varies across latitude, with cooler temperatures represented in maroon on the left and warmer temperatures in yellow on the right.

shifts may drive or be driven by shifts in microbial functioning. For example, plant communities dominated by acquisitive traits (such as high specific leaf area (SLA) and nitrogen-rich leaves) correspond with bacterial metabolic pathways that yield faster rates of decomposition and nutrient cycling, slower rates of C sequestration[30,33,34] and promote arbuscular mycorrhizal fungal associations or reduced dependence on mycorrhizal associations[35,36]. In contrast, communities dominated by more conservative traits (for example, low-SLA and nitrogen-poor leaves) tend to be associated with less fertile soils that limit microbial metabolism, resulting in slower rates of decomposition and nutrient cycling[3,30,34,37] and promoting ectomycorrhizal fungal associations[19,35,36,38]. Colder and/or shorter growing seasons are expected to select for more conservative leaf traits that buffer leaf temperatures relative to air temperatures and promote increased rates of net photosynthesis and plant growth[24,39]. Thus, across a broad temperature gradient, variation in plant functional trait composition may inform understanding of plant–microbe interactions and their influence on soil nutrient cycling and decomposition.

Building on this framework (Fig. 1), we take an integrative approach to assess three prominent hypotheses: (1) the soil-substrate age hypothesis (SSH)[28,40,41], (2) the growth rate hypothesis (GRH)[39,42–44], and (3) the adaptive trait continuum hypothesis (ATH)[45,46]. The SSH posits that tropical soils are P-limited as a result of increased leaching due to high rainfall and old soil age, whereas higher latitude soils are N-limited[28,47].The GRH links the elemental composition of organisms to their metabolic rates where species with rapid growth have decreased N:P ratios due to increased tissue P-content as the result of increased allocation to P-rich ribosomes for protein synthesis[39,42–44]. The GRH has important implications for understanding variation in trait composition and nutrient cycling across broad temperature gradients[39]. For example, GRH states that in increasingly colder climates, selection to counteract the kinetic effects of temperature on growth selects for more leaf P relative to leaf N (refs. [43,45]). Both hypotheses predict an increase in plant tissue N:P ratio with increases in decreased latitude and higher temperatures. This shift in plant leaf N:P ratio influences the functioning of soil microbes by altering the relative inputs of either N or P into the system, leading to reduced microbial biomass in N-limited regions and reduced microbial metabolism in P-limited regions[48]. Building on the GRH, the ATH states that shifts in trait composition and diversity reflect selection for optimal matching of phenotypes with local climate[45,46]. Therefore, it is not only important to understand how individual traits vary across environmental gradients but to assess the combination of traits in a community. These hypotheses provide a predictive framework for describing plant-trait distributions that can be applied to understanding and predicting microbial-trait distributions related to nutrient cycling.

In this study, we quantify variation in the dominance of both plant and microbial functional traits to assess proposed mechanisms underlying shifts in species assemblages across temperature. We examined 19 bacterial traits and 13 fungal traits (represented by functional genes; Supplementary Table 1) from 30 soil microbial communities from 1,134 soil cores (Supplementary Table 1) and four plant leaf traits (SLA, N:C ratio, N:P ratio and δ^{15}N; Supplementary Table 1) from 30 vegetative plots at six sites spanning a large latitudinal temperature gradient as characterized by mean annual soil temperature (MAST; Supplementary Fig. 1).

Results

Soil-substrate age hypothesis and growth rate hypothesis. First, we evaluated the SSH and GRH for how key traits related to C-, N- and P-cycling in plants, bacteria and fungi vary across temperature and latitude. For plants, we observed an overall shift in the community-weighted mean (CWM) trait value from more conservative traits (thick, dense leaves) in more variable cold climates to more acquisitive traits (thin, less dense leaves) in more stable climates (SLA $r^2=0.636$, $P<0.0001$ and N:C ratio $r^2=0.693$, $P<0.0001$; Fig. 2a,d). As soil C increases in colder climates (see Supplementary Table 2), bacterial and fungal CWM traits for C degradation of pectin (rhamnogalacturonan lyase, *RGL*) showed opposite relationships, significantly decreasing for bacteria (*RGL* $r^2=0.611$, $P<0.0001$; Fig. 2b) and increasing for fungi (*RGL* $r^2=0.326$, $P=0.001$; Fig. 2c) with increased MAST. Leaf CWM δ^{15}N increased significantly with MAST ($r^2=0.713$, $P<0.0001$; Fig. 2g). Four of the six bacterial functional traits related to N cycling decreased significantly with increased MAST (Supplementary Table 3 and Fig. 2h). Furthermore, fungal functional traits associated with denitrification (*nirK*) and P degradation (*ppx*) were significantly greater in the tropics (Supplementary Table 3 and Fig. 2l).

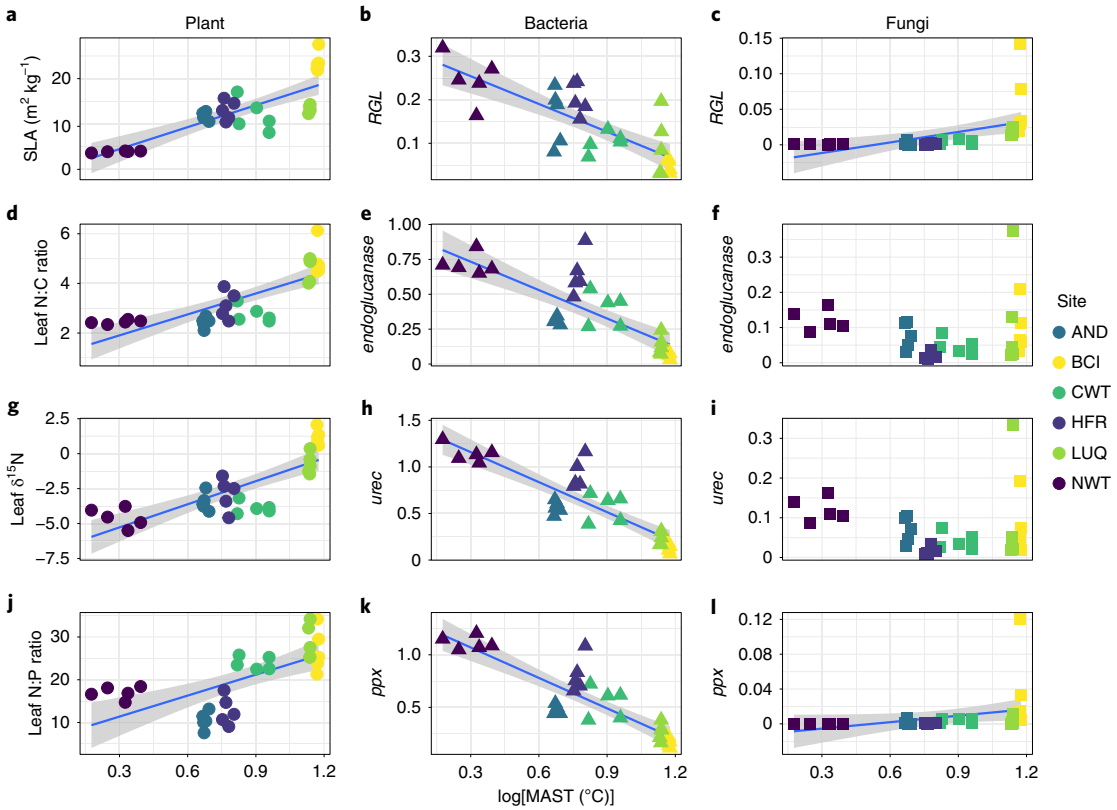

Fig. 2 | Shifts in community-weighted leaf and microbial traits that influence soil nutrient availability across 30 forest plots at six sites spanning a broad latitudinal temperature gradient. a, SLA as a function of the natural log of MAST (lnMAST, °C). **b**, Rhamnogalacturonan lyase (*RGL*, a carbon degradation gene) of bacteria as a function of lnMAST. **c**, *RGL* of fungi as a function of lnMAST. **d**, Leaf N:C ratio as a function of lnMAST. **e**, Endoglucanase (*endoglucanase*, a carbon degradation gene) of bacteria as a function of MAST. **f**, *endoglucanase* of fungi as a function of lnMAST. **g**, Leaf nitrogen isotope (δ^{15}N) as a function of lnMAST. **h**, Urease alpha subunit (*ureC*, a nitrogen gene associated with ammonification) of bacteria as a function of lnMAST. **i**, *ureC* of fungi as a function of lnMAST. **j**, Leaf N:P ratio as a function of lnMAST. **k**, Exopolyphosphatase (*ppx*, a phosphorus degradation gene) of bacteria as a function of lnMAST. **l**, *ppx* of fungi as a function of lnMAST. Circles, plant traits; triangles, bacterial traits; squares, fungal traits. Solid blue line, linear regression for significant relationships ($P < 0.05$). Grey area, standard error of the linear regression. Site abbreviations: AND, HJ Andrews Experimental forest; BCI, Barro Colorado Island; CWT, Coweeta LTER; HFR, Harvard Forest; LUQ, Luquillo LTER; NWT, Niwot Ridge LTER.

We found an increase in ectomycorrhizal associations in temperate regions (Supplementary Table 4). Furthermore, the leaf CWM N:P ratio increased with MAST (Fig. 2j; $r^2 = 0.463$, $P > 0.0001$) and decreased with latitude ($r^2 = 0.596$, $P > 0.0001$) where 20 of the 30 plots had values of leaf N:P ratios greater than 15.

Adaptive trait continuum hypothesis. To evaluate the ATH, we assessed shifts in multivariate trait space for plant, bacterial and fungal functional traits across MAST. We conducted principal components analyses for traits related to C-, N- and P-cycling using CWMs for plant, bacteria and fungi. Principal component 1 (PC1) accounted for 76.4% of the variation in plant functional traits, 56% of the variation in bacterial functional traits and 55.8% of the variation in fungal functional traits (Fig. 3; biplots are in Supplementary Figs. 2–4). Consistent with the ATH, plants and bacteria (but not fungi) showed pronounced, directional shifts in multivariate functional trait space across this broad soil temperature gradient (Fig. 3). The natural log of MAST explained a large proportion of the variation in plant (Fig. 3a; $r^2 = 0.825$, $P > 0.0001$) and bacterial (Fig. 3b; $r^2 = 0.754$, $P > 0.0001$) functional traits. These shifts in microbial and plant functional diversity were more strongly correlated with soil temperature than with soil moisture (Supplementary Table 5).

Next, we used simple linear regression, multiple linear regression and piecewise structural equation modelling to explore relationships between soil environment, microbial functional traits and plant functional traits (Table 1). In these models, all dependent and independent variables are PC1 scores that characterize variation in soil environment variables (*S*), bacterial functional traits (*B*), fungal functional traits (*F*) and plant functional traits (*P*).

First, we build on the ATH to evaluate how the local soil environment as measured through key variables (PC1 of MAST, mean annual soil moisture (MASM) and pH; Supplementary Fig. 5) drive variation in microbial and plant functional traits. This was supported by simple regression models 1–3 (Table 1), which showed that functional traits of plants, bacteria and fungi varied significantly with the soil environment (all $P \leq 0.05$). The soil environment explained 74% of the observed variation in plant functional traits, 64% of the observed variation in bacterial functional traits and 13% of the observed variation in fungal functional traits, suggesting that plant functional traits followed by bacterial functional traits are more strongly associated with soil environment variables than are fungal functional traits.

Next, building from models 1–3 (Table 1), we constructed multiple regression models that use soil environment and functional traits as covariates for predicting variation in plant, bacterial and fungal functional traits (models 4–7, Table 1). For models predicting functional variation for each clade, inclusion of functional covariates gave similar results to those of models 1–3 (Table 1) without a significant preference for the multiple regression models over their simple regression counterparts.

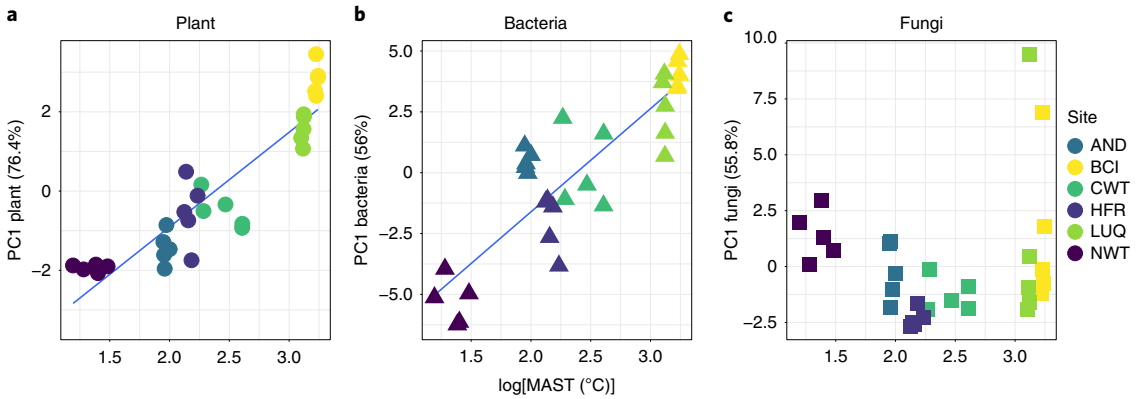

Fig. 3 | Adaptive trait continuum for plants and microbes spanning a broad latitudinal temperature gradient. a, PC1 from principal component analysis of plant traits related to growth, nutrient availability and decomposition as a function of the natural log of MAST (lnMAST, °C). **b**, PC1 for bacterial traits related to nutrient cycling as a function of lnMAST. **c**, PC1 for fungal traits related to nutrient cycling as a function of lnMAST. Symbols and site abbreviations as in Fig. 2. Solid blue line, linear regression for significant relationships ($P < 0.05$).

On the basis of multiple regression results (models 4–7, Table 1), we used piecewise structural equation models (piecewise SEM, refs. [49,50]) with second-order Akaike information criterion (AICc) model selection[51] to explore directional causal relationships between variables. The multiple regression models 4–7 were written as SEMs with soil PC1 as the exogenous variable (models 8–11, Table 1). Most SEMs were preferred (all AICc ≤ 32, except models 10 and 15) over their simple and multiple regression counterparts. For models comprising bacterial traits and plant traits (models 8–9), d-separation[51] identified missing paths between soil environment and plant traits (model 8) or soil environment and bacterial traits (model 9). For both models, inclusion of missing paths and removal of non-significant paths yielded model 12 ($r^2_{S\rightarrow P} = 0.74$, $r^2_{S\rightarrow B} = 0.64$; Fig. 4a and Table 1), which is the preferred model combining plant traits and bacterial traits (AICc = 22). This model indicates that variation in the soil environment independently drives both plant functional traits and bacterial traits. For models considering fungal traits and plant traits (models 10–11, Table 1), there were no significant paths between fungal and plant traits and d-separation[51] identified missing paths between soil environment and plant traits (model 10) or fungal traits (model 11). For both models, inclusion of missing paths and removal of non-significant paths gave model 13 ($r^2_{S\rightarrow P} = 0.74$; Table 1), which is the preferred model on the basis of fungal and plant traits (AICc = 7). This model indicates that there are no causal pathways between fungal traits and plant traits or soil environment. The resulting model excludes fungi, emphasizing the relationship between the soil environment and plant traits and suggesting that variation in plant traits is independently driven by variation in the soil environment (Fig. 4b,e).

We constructed two more (14 and 15, Table 1) that examine potential relationships between soil, bacteria and fungi only (these models do not consider plant functional trait variation). Consistent with simple linear regression models 2 and 3 (Table 1), models 14 and 15 showed that variation in soil environment was a significant predictor of variation in bacterial and fungal functional traits, respectively. However, these models also indicated that there were no significant paths between bacterial and fungal traits and d-separation[51] identified additional missing paths between soil environment and fungal traits (model 14) or bacterial traits (model 15). For both models 14 and 15, inclusion of missing paths and removal of non-significant paths gave models 16 and 17, respectively. Of these models, AICc model selection identified model 17 ($r^2_{S\rightarrow B} = 0.73$, $r^2_{F\rightarrow B} = 0.25$; Fig. 4c and Table 1) as the preferred model combining bacterial and fungal functional traits (AICc = 10). Model 17 indicates that when plant functional traits are not considered, variation in bacterial functional traits is independently driven by variation in soil environment and fungal functional traits and there are no significant pathways between soil environment and fungal traits (Fig. 4c,f).

Discussion

This study assessed a central hypothesis of trait-based ecology—namely that temperature drives shifts in functional traits associated with decomposition and nutrient availability to ultimately influence ecosystem processes[23,28,39,45,52,53]. The latitudinal diversity gradient provides a platform for empirically testing trait-based hypotheses for nutrient availability (SSH)[28,47], nutrient cycling via the kinetic effects of temperature on growth (GRH)[39] and finally how temperature shapes the optimal phenotype (ATH)[45]. These hypotheses provide a predictive framework for describing plant traits across a broad temperature gradient and applying them to characterize shifts in key microbial traits provides a more thorough understanding of nutrient availability and cycling (Fig. 1). Also, this integrative approach provides insight to how abiotic factors drive variation in the multivariate trait composition of plants and microbes, which may result in direct and/or indirect ecological feedbacks. These biotic interactions may be characterized as shifts in microbial functional trait composition driven by shifts in plant functional trait composition, or as shifts in plant functional traits driven by shifts in microbial traits. While these interactions may not be mutually exclusive, both influence soil properties and chemistry, further shaping feedbacks between organisms and their environment.

Soil-substrate age hypothesis. The SSH comes from the observation that soil nutrient content changes with soil age from weathering and leaching, and posits that tropical soils are P-limited due to increased leaching and old age, whereas higher latitude soils are N-limited[28]. We found associated changes in plant resource acquisition strategies with changes in nutrient availabilities. Specifically, in support of the SSH, we observed that leaf N:P ratios generally decreased with latitude and increased with temperature. However, 20 of the 30 plots had values of N:P ratio greater than 15, suggesting that plots in Colorado and North Carolina may also be P-limited[28,30,54]. Furthermore, we examined CWM leaf δ^{15}N as an integrative measure of total N-cycling (where more negative leaf δ^{15}N corresponds to lower N availability and more N-fixing microbial associations[53,55]) and found it increased with MAST. Overall, the low levels of leaf δ^{15}N observed for temperate regions further supports the proposed N-limitation at higher latitudes and colder

Table 1 | Models exploring drivers of variation in microbial and plant functional traits that are relevant for ecosystem nutrient cycling

Model	Path diagram	*P*	r^2 or adjusted R^2	AICc
Simple linear regression models				
1		9.08×10^{-10}	0.74	50
2		1.04×10^{-7}	0.64	60
3	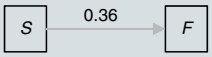	0.05	0.13	87
Multiple linear regression models				
4		2.40×10^{-9}	0.75	50
5	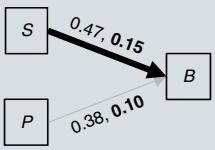	2.18×10^{-7}	0.66	60
6		3.22×10^{-9}	0.75	50
7		0.05	0.14	87
8	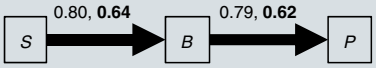	0 (NS)	NA	32
9	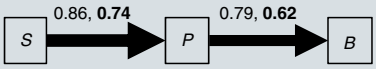	3.7×10^{-2} (NS)	NA	22
10	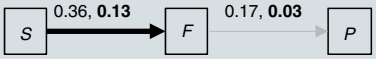	0 (NS)	NA	57
11		0.02 (NS)	NA	23
12	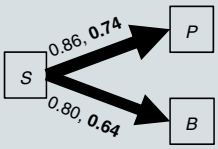	0.09	NA	**21**
13		1.0	NA	**7**
14	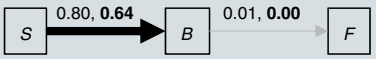	1×10^{-3}(NS)	NA	30
15		0 (NS)	NA	55

(Continued)

Table 1 | Models exploring drivers of variation in microbial and plant functional traits that are relevant for ecosystem nutrient cycling (continued)

Model	Path diagram	*P*	r^2 or adjusted R^2	AICc
16	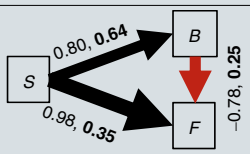	1.0	NA	19
17	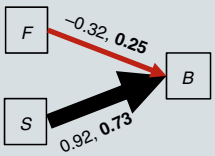	1.0	NA	**10**

The models use PC1 scores that characterize variation in soil environment variables (S), bacterial functional traits (B), fungal functional traits (F), and plant functional traits (P). Bolded numbers in the Model and AICc columns indicate the preferred model obtained via d-separation and/or AICc model selection. In the path diagrams, boxes represent measured variables and arrows represent unidirectional relationships between variables. Black arrows represent positive relationships, red arrows represent negative relationships, and grey arrows represent non-significant paths at $\alpha = 0.05$. Non-bolded numbers are standardized effect sizes, and bolded numbers are coefficients of determination (r^2; partial r^2 reported for multiple linear regressions). Arrow thickness has been scaled according to standardized effect sizes. NS, not non-significant relationship at $\alpha = 0.05$; NA, not applicable.

climates, suggesting ectomycorrhizal associations may be favoured in these regions. Indeed, we found an increase in ectomycorrhizal associations in temperate regions (Supplementary Table 4). Increased ectomycorrhizal associations facilitate decomposition of the more recalcitrant leaf litter associated with slow-conservative leaf traits[35,56]. In addition to shifts in mycorrhizal associations, a fungal functional trait associated with denitrification (*nirK*) was found to be significantly greater in the tropics (Supplementary Table 3), supporting the SSH which predicts an increase in N availability in lower latitudes that may further correspond with fewer ectomycorrhizal associations in these regions. Most bacterial functional traits related to N-cycling significantly decreased with increased MAST, which may reflect fewer enzymatic active sites in tropical systems as the result of increased availability of more labile substrates for extraction and use by bacteria.

Growth rate hypothesis. The GRH predicts that species with rapid growth have decreased N:P ratios due to increased P-content of tissues as the result of greater allocation towards P-rich ribosomes for protein synthesis[39,42–44]. In ecosystems with cold, short growing seasons, selection for more rapid growth rates result in more species with higher P irrespective of P limitations. However, if the system is both P-limited and there is less selective pressure for fast growth rates then plants should have increased N:P ratios[39,42–44]. Compared to colder forests, warmer forests have trees with canopies with low foliar C and P but higher N content, as supported by the observed increase in N:P ratios with increased temperature. Additionally, the observed shift in soil nutrient availability (N:C ratio; Supplementary Table 2) is supported by an increase in CWM leaf δ^{15}N with temperature, indicating that tropical ecosystems are more N-rich with higher rates of litter decomposition (increase in leaf N:C ratios) that are matched with more acquisitive plant traits (increase in SLA)[55]. This functional shift is matched by soil bacteria with overall higher capacities for C, N and P use in cooler climates, possibly driven by a combination of substrate availability and complexity. For example, temperate soils are large C reserves, where the high complexity of C substrates result in lower rates of decomposition that may require increased affinity of bacterial functional traits associated with C-cycling. Similarly, N limitation in temperate climates may result in higher capabilities of N degradation to effectively use the low biologically available nutrient (Fig. 2b,e,h,k and Supplementary Table 1). However, we observed an opposite pattern for fungi, suggesting they have a greater (albeit more variable) capacity for C (*RGL* increased with MAST), N (*nirK* increased with MAST) and P (*ppx* increased with MAST) use in warmer climates despite nutrient limitations (Fig. 2c,l and Supplementary Table 3, *nirK*). This suggests that bacteria and fungi differentially contribute to nutrient cycling across the gradient and may respond differently to changes in climate.

Adaptive trait continuum hypothesis. Building on the ATH[45], if the latitudinal diversity gradient represents a change in species richness[57–59], then we expect a change in the phenotypic optimum that necessitates a change in community trait distribution[45]. We can further make predictions for how traits should shift from more conservative in lower temperatures of high latitudes to more acquisitive in higher temperatures of lower latitudes. Although we assessed traits individually and observed clear shifts in the conservative-acquisitive continuum with temperature, consistent with the leaf economic spectrum hypothesis[52,60,61], changes in multivariate trait space provide an integrative understanding of how the phenotypic optima change with temperature. We documented shifts in multivariate functional trait space across the temperature gradient for plants and bacteria that ultimately reflect changes in life history, genetic variation and community variation[46]. In contrast to recent findings[21], we found a stronger relationship between traits of plants and bacteria than those of plants and fungi. Although we did not observe a significant shift in the multivariate trait space for fungi, this may suggest that soil temperature is not a key driver in fungal traits across the latitudinal gradient, and that other abiotic or biotic properties may be more important for shaping fungal trait distributions[35,53]. It is also possible that this lack of relationship for fungi is the result of the functional traits measured in this study, suggesting that other plant or fungal trait combinations may be better predictors. For example, given the importance of mycorrhizal fungi in the rhizosphere, and relationships between the rhizosphere and climate, it is possible that plant root traits and/or fungal morphological traits are more closely associated with temperature gradients[62].

Conclusion

Variation in leaf traits directly affects soil-substrate quality, which in turn influences microbial activity and biogeochemical processes[31]. Although our understanding of how plant traits influence these processes is still developing, few studies have assessed couplings of plant and microbial functional traits across broad environmental gradients[63]. For example, shifts in microbial functional composition could be driven by shifts in plant functional trait composition[63]. Alternatively, shifts in plant functional traits could be influenced by shifts in microbial traits that in turn influence

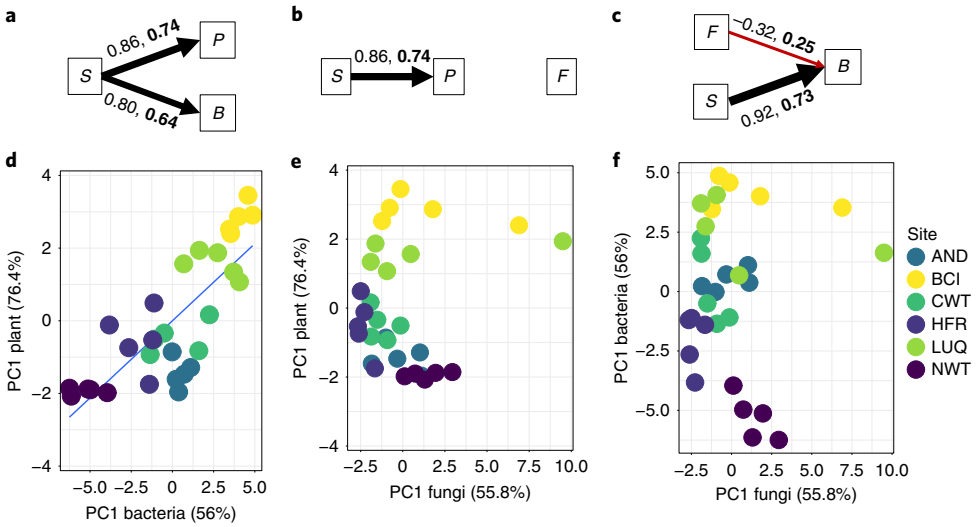

Fig. 4 | Relationships between microbial and plant functional traits that are relevant for ecosystem nutrient cycling. a–c, Best-fit structural equation models (SEMs) exploring drivers of variation in microbial and plant functional traits. **a**, Best-fit SEM (model 12, Table 1) of the soil environment (*S*) on bacterial traits (*B*) and plant traits (*P*). **b**, Best-fit SEM (model 13, Table 1) of *S* on fungal traits (*F*) and *P*. **c**, Best-fit SEM (model 17, Table 1) of *S* on *F* and *B*. **d**, Principal component 1 (PC1) from the principal component analysis of plant functional traits as a function of PC1 from the principal component analysis of *B* ($r^2 = 0.621$). **e**, PC1 from the principal component analysis of *P* as a function of PC1 from the principal component analysis of *F*. **f**, PC1 from the principal component analysis of *B* as a function of PC1 from the principal component analysis of *F*. In **a–c**, boxes represent measured variables and arrows represent unidirectional relationships between variables. Black arrows represent positive relationships, and red arrows represent negative relationships. Non-bold numbers are standardized effect sizes and bold numbers are coefficients of determination (r^2; partial r^2 reported for multiple linear regressions). Arrow thickness has been scaled according to standardized effect sizes. In **d–f**, PC1 from the principal component analysis of *B* as a function of PC1 from the principal component analysis of *F*. Blue line, linear regression for significant relationships ($P < 0.05$). Site abbreviations as in Fig. 2.

soil properties and chemistry. Our results demonstrate the pathways of causality linking soil climate, microbial traits and plant traits (Table 1) and highlight coordinated shifts in both plant and microbial functional trait diversity across a broad latitudinal temperature gradient (Fig. 4). Together, these results support a key premise of trait-based ecology, where correlated variation in plant and bacterial functional traits linked to ecosystem processes are driven by temperature[63]. Changes in soil properties across the temperature gradient drive variation in plant functional traits and bacterial functional traits (Fig. 4a) reflecting nutrient limitation across broad ecological gradients[28] and highlighting the regional effects of biogeochemical processes, microclimates and energy fluxes on microbial diversity[10,32,33,64]. However, fungal taxonomic and functional diversity are considerably less understood than both plants and bacteria, which may result in unobserved relationships and inexplicit biases.

Our findings underscore the importance of temperature in structuring the coupling of plant and microbial functional diversity in and across forest ecosystems, as well as for biogeochemical cycling. As a result, they have implications for understanding and predicting ecological consequences of climate change. First, if temperature drives the observed shift in plant and bacterial functioning from tropical to subalpine forests, ecosystems subjected to climate warming should also experience directional shifts in functional diversity and biogeochemistry. Our results provide comparisons of functional traits in and across bacterial, fungal and plant communities spanning a latitudinal temperature gradient. They also point to the importance of a trait-based approach for providing powerful tools and measures for projecting the effects of current and future climate warming[6,7,10,65,66].

Although several challenges remain in fully comparing patterns of functional traits across taxonomic groups, our findings highlight the mechanisms that help shape biodiversity across temperature and further increase our understanding of the main drivers that structure and maintain diversity gradients. Limits on our ability to identify and quantify activity of microbes remain an outstanding challenge. Due to the complex and heterogeneous nature of soil, biases may be present during many steps of processing for sequencing, such as DNA extraction, PCR amplifications and primers[67–70] leading to over/under-representation of certain taxa. Another challenge is that the presence of a gene in an organism does not necessarily mean that the gene is expressed. With the major advances in molecular tools, continued collections of in situ samples across broad environmental gradients will provide more insights to the mechanisms driving patterns of functional diversity across trophic levels.

Methods

Study system. We collected data from six forest sites along a broad latitudinal temperature gradient from 9 to 44° N (Supplementary Fig. 1a). Five sites are part of the National Science Foundation (NSF) Long-Term Ecological Research (LTER) network: Niwot Ridge, Colorado (NWT); Harvard Forest, Massachusetts (HFR); H. J. Andrews Experimental Forest, Oregon (AND); Coweeta, North Carolina (CWT); Luquillo, Puerto Rico (LUQ). The sixth site, Barro Colorado Island, Panama (BCI) is administered by the Smithsonian Tropical Research Institute. The selected sites characterize variation from subalpine to temperate to tropical forest ecosystems, and span broad climate gradients, with mean annual temperatures ranging from 2.5 to 25.7 °C and mean annual precipitation ranging from roughly 500 to 3,100 mm (Supplementary Fig. 1b). At each of these locations, a permanent 25-ha plot was established from which all sampling for woody plants and soil microbes occurred. Each 500 × 500 m^2 (25 ha) plot was oriented north (Supplementary Fig. 6a). In each plot, we established five 0.1 ha 'Gentry' style vegetation plots that consisted of five 100 × 2 m^2 transects and 21 individual square-metre soil plots. Each 100 m transect of the vegetation plots was divided into two 50 m segments and was separated by 8 m from the next 100 m transect, so that each 'Gentry' plot was located in a 42 × 100 m^2 area (Supplementary Fig. 6b). The 21 square-metre soil plots were laid out on perpendicular transects (Supplementary Fig. 6c) with plots adjacent to 1, 10, 50, 100 and 200 m in each cardinal direction from a central square-metre plot. During the autumn of 2011 and spring on 2012, all woody vegetation greater than 1 cm at ground height was measured, identified and tagged.

At each site, we also collected and homogenized nine surface-soil cores (~10 cm depth, Oakfield Apparatus Company model HA) from 21 square-metre plots in the summer of 2012 (1,134 soil cores in total).

Plant functional traits. We collected five leaves from at least two individuals of the five most abundant species on the basis of their basal area in each plot at each site and averaged trait values at the genus level in each plot to match microbial level measurements (76 unique genus across sites; Supplementary Table 6). We measured four leaf traits related to resource acquisition, nutrient availability and biogeochemical cycling to characterize plant functional diversity: SLA, δ^{15}N, leaf N:P ratio and leaf N:C ratio[6,27,28,32]. For each leaf, the fresh leaf area was measured using a flatbed scanner and the area was calculated using image analysis software ImageJ. Leaves were dried in a drying oven for a minimum of 72 h at 60 °C before the final dry mass was weighed. Leaves were then transported dry to the University of Arizona where they were placed again into a drying oven and ground into a fine homogenous powder for leaf stoichiometry and isotope assays. Total P concentration was determined using persulfate oxidation followed by the acid molybdate technique (APHA 1992) and P concentration was then measured colorimetrically with a spectrophotometer (ThermoScientific Genesys20). Concentrations of δ^{15}N, C and N were measured by the Department of Geosciences Environmental Isotope Laboratory at the University of Arizona on a continuous-flow gas-ratio mass spectrometer (Finnigan Delta PlusXL) coupled to an elemental analyser (Costech). Samples of 1.0 ± 0.2 mg were combusted in the elemental analyser. Standardization is on the basis of acetanilide for elemental concentration, NBS-22 and USGS-24 for δ^{13}C and IAEA-N-1 and IAEA-N-2 for δ^{15}N. Precision is at least ± 0.2 for δ^{15}N (‰), on the basis of repeated internal standards. We used four traits related to resource acquisition, nutrient availability and biogeochemical cycling to characterize plant functional diversity: SLA, δ^{15}N, leaf N:P ratio and leaf N:C ratio[71]. SLA is defined as the light-capturing surface area per unit of dry mass ($m^2 kg^{-1}$)[72,73]. SLA has been shown to correlate with net photosynthetic capacity, leaf longevity, relative growth rate, litter decomposition and nutrient cycling[6,27,72,74]. Stable nitrogen isotope (δ^{15}N, ‰) describes the ratio of ^{15}N to ^{14}N in foliar tissue[75]. Leaf δ^{15}N has been used as an integrative measure of N cycling[55]. Variation in the ratio of ^{15}N and ^{14}N provides information on the differences in N acquisition and origin N. Furthermore, it has been shown to be positively correlated with N-fixing microbial associations[76]. Leaf N:P ratio reflects shifts in the allocation of N towards rubisco for photosynthesis and P towards ribosomal RNA for protein synthesis and has been shown to decrease with latitude[28,77]. Leaf N:C ratio reflects shifts between carbohydrates and proteins in leaf tissue and is a good predictor of decomposition rates[78–80]. To be consistent with methods used for microbial analyses, observations for many species within each genus were averaged to create a genus-level mean trait value for each plot. This only occurred when many measurements per species per genus were available in a plot.

DNA extraction. Community DNA was extracted using a grinding SDS lysis extraction methods followed by gel purification as described previously[81] from 5 g of mixed soils from nine sampling cores pooled from each square-metre plot. DNA quality was assessed using NanoDrop ND-1000 Spectrophotometer (NanoDrop Technologies). DNA concentration was measured by PicoGreen using a FLUOstar OPTIMA fluorescence plate reader (BMG LABTECH).

Sequencing methods. Specific PCR was performed to amplify soil community DNA using primers of the V4 region of 16S rRNA genes for bacteria and internal transcribed spacer (ITS) between 5.8S and 28S rRNA genes for fungi as described previously[58]. PCR amplicons were sequenced by an Illumina MiSeq sequencer. The raw reads of 16S and ITS were processed as previously reported[58]. Pair-end sequences were joined with FLASH (ref. [82]). Unqualified sequences were filtered by Btrim program[83]. U-CHIME (ref. [84]) was used to remove chimeras before operational taxanomic unit (OTU)s were obtained by UCLUST at the 97% sequence identity[85]. Representative sequences of OTUs were aligned PyNAST (refs. [86,87]) for 16S and MUSCLE (ref. [88]) for ITS. The alignments were then used to construct an approximately maximum-likelihood phylogenetic tree using FastTree2 program[89]. Taxonomic identity of each representative sequence was determined using the RDP Classifier[90] and chloroplast, mitochondria and archaeal sequences were removed from 16S dataset. In addition, singletons detected solely in one of the subsamples were discarded before the statistical analyses to remove noise from the dataset. After the OTU table was generated, we rarefied each sample to the sequencing depth of 25,901 per sample for 16S and 13,688 per sample for ITS. To address concerns that arise with the use of rarefied data, we did a simulation to compare the accuracy of CWM calculated after normalization by different methods. DESeq or edgeR was recommended to replace rarefying[91]. Isometric log-ratio, additive log-ratio and centred log-ratio are recommended considering compositional data issues[92]. Since isometric and additive log-ratios are not applicable to CWM calculation (data cannot match taxa trait after transform), we compared rarefying with centred log-ratio, DESeq, edgeR and proportion without rarefying. To simulate a local community, we randomly draw 10,000 OTUs from the phylogenetic tree observed in our study. Then, the trait of each OTU, defined as the optimum environmental condition for each OTU, is simulated as a Brownian motion model of evolution. The individual number (total abundance) is 1×10^8, which is close to the total number of bacterial cells in 1 g of soil. The abundance of each OTU depends on the fitness (that is, difference of the trait and environmental condition) and is calculated using a Gaussian function. The CWM value calculated from the 1×10^8 individuals is the expected 'true' CWM. We simulated sequencing results with different library sizes (sequencing depth, from 1×10^2 to 5×10^5) as random draw from the 1×10^8 individuals. Then, the simulated sequencing results are normalized by different methods and CWM is calculated after normalization. The R code and tree file are available as Supplementary Data 4. The results (Supplementary Fig. 7) demonstrated: (1) rarefying led to accurate estimation of CWM across all tested library sizes; (2) rarefying to 100 reads showed higher standard deviation of CWM than other methods but rarefying to 10,000 reads obtained high precision without obvious standard deviation; (3) DESeq and edgeR resulted in obviously incorrect CWM unless the library size is large enough; (4) centred log-ratio totally transformed the data, thus always miscalculating CWM. The results indicate the 'rarefying and compositional issue' is not a notable problem for CWM calculation and current recommended solutions to the issue are not applicable or necessary for CWM calculation. The OTU tables are available at http://www.ou.edu/ieg/publications/datasets and the raw sequencing data have been deposited in the NCBI Sequence Read Archive under accession code PRJNA308872. On the basis of the rarefied OTU table, we calculated relative abundance of each OTU in each sample (ϕ_{il}) and average relative abundance of each OTU in each site (ϕ_{ik}).

GeoChip hybridization and data processing. The purified DNA was analysed by GeoChip 5.0. DNA labelling, hybridization and imaging were performed as previously described[93,94]. The raw GeoChip data were preprocessed using a data analysis pipeline (http://ieg.ou.edu/microarray/). Outliers and unreliable signals were identified by the microarray imaging software (Agilent) and removed before further analysis. The raw data were normalized across samples by the sum of target spot signals and unqualified spots (for example, signal-to-noise ratio less than 2.0) were removed. The within-array normalization was performed on the basis of signals of universal standards. Across all samples, spot signals were normalized by the average signal intensity of control spots and then by the sum of all sample spot signals. Next, the spots with: (1) a signal-to-noise ratio less than 2.0, (2) a coefficient of variation larger than 0.8, or (3) a raw signal less than 100 were removed as unqualified readings. The qualified signals in each sample were logarithmic transformed and divided by the mean of qualified signals in the sample to get final signals of target spots. Each target spot represents a probe, that is a functional gene in a certain type of microorganisms, usually a gene in a certain species, subspecies or strain. In this study, we focused on the probes of functional genes involved in the cycling of C, N and P (Supplementary Table 1). For each functional trait represented by a certain gene (trait j), we identified all probes of gene j belonging to a certain taxon (taxon i) and calculated the average signal of detected probes in a certain plot (plot l) to measure the functional trait j of taxon i in plot l (λ_{ijl}). We also calculated a probe signal in each site as the sum of the probe signal across all samples from the site. Then, for gene j, the average signal of all probes belonging to taxon i in a site (site k) was used to measure the functional trait j of taxon i in site k (λ_{ijk}). The microarray data presented are available at http://www.ou.edu/ieg/publications/datasets.

Mycorrhizal associations. Mycorrhizal associations were categorized using Nguyen et al. for fungi and Wang and Qiu[95,96]. Mycorrhizal associations included arbuscular mycorrhiza, ectomycorrhiza, ericoid mycorrhiza (trees only) and their combinations calculated as percentages. Percentage was calculated on the basis of taxon abundance for arbuscular mycorrhiza, ectomycorrhiza and all mycorrhiza (Supplementary Table 4).

Analysis. All analyses were performed using the statistical software R. To characterize patterns of functional traits across temperature, we calculated abundance weighted community level trait metrics using genus abundances in each site k for each trait j. CWM_{jk} was calculated for each site k for each trait j as:

$$\mathrm{CWM}_{jk} = \Sigma \phi_{ik} \lambda_{ijk} \quad (1)$$

where ϕ_{ik} is the relative abundance of taxa i in site k, λ_{ijk} is the trait mean of taxa i in site k. CWM_{jl} was calculated for each plot l for each trait j as:

$$\mathrm{CWM}_{jl} = \Sigma \phi_{il} \lambda_{ijl} \quad (2)$$

where ϕ_{il} is the relative abundance of taxa i in plot l, λ_{ijl} is the trait mean of taxa i in plot l. This metric is commonly used in trait-based community ecology in plants but has never been applied to microbial communities. To apply it to microbial communities, we make three general assumptions (Supplementary Box 1). First, for each soil sample, we used the output from GeoChip data for each functional gene as a measure of gene abundance per gene per taxa[69,97,98]. An assumption of this approach is that GeoChip output corresponds to microbial functional capacity (ranging from low to high capacity). If the presence of a functional gene has a low occurrence value obtained using GeoChip then that taxon has a low capacity for that function (low potential rate of corresponding reaction per unit of microbial biomass). Second, the taxa detected by both sequencing and GeoChip analysis

may represent the major taxon with the function of interest due to greater genomic coverage of more common taxa. Third, 16S and ITS sequencing results can be used to measure the relative abundances of taxa. Results of 16S and ITS sequencing are now widely serving as practical measures of taxa relative abundances. Although amplicon sequencing has reproducibility issues, current amplicon sequencing can still be useful and obtain acceptable (though relative) reliability if used appropriately. To ensure appropriate use, we set standard biological replicates, remove singletons and used abundance rather than binary results[67,99].

To evaluate the relationships between CWM_{jl} traits for plants, microbes and MAST, a linear regression was performed using the lm function in base R. To assess the multivariate trait space, a principal component analysis was conducted on the standardized CWM_{jl} data using the prcomp function in base R. Linear regression was used to assess the relationship between PC1 and MAST for plants, bacteria and fungi. PC1 for both bacteria and fungi were then compared to PC1 for plant traits using linear regression. We used simple linear regression, multiple linear regression and piecewise structural equation modelling to explore relationships between soil environment, microbial functional traits and plant functional traits (Table 1). In these models, all dependent and independent variables are standardized PC1 scores that characterize variation in soil environment variables, bacterial functional traits, fungal functional traits and plant functional traits. We evaluated the hypothesis that soil environment variables (MAST, MASM and pH) are primary drivers of variation in microbial and plant functional traits by using the PC1 for the soil environment. AICc was used to indicate the preferred model obtained via d-separation and/or AICc model selection. Path diagrams were created to represent the relationship between measured variables (for example, PC1 for soil, plants, bacteria and fungi) with arrows that represent the unidirectional relationships between those variables, with significance set to $\alpha = 0.05$. Standardized effect sizes and coefficients of determination (r^2; partial r^2 reported for multiple linear regressions) were calculated and used to scale the arrows.

Relative importance of explanatory variables was conducted to explore the relationship between MAST and MASM. A multiple linear regression in the form of (trait = a + soil temperature (x) + soil moisture (x)) was used to determine importance of soil temperature compared with soil moisture. The R package relaimpo was used to calculate the relative importance of MAST and MASM on each CWM trait as well as each PC1 for plants, bacteria and fungi[100] (Supplementary Table 5).

Reporting Summary. Further information on research design is available in the Nature Research Reporting Summary linked to this article.

Data availability

Raw sequencing data have been deposited in the NCBI Sequence Read Archive under accession code PRJNA308872. The OTU tables and microarray data presented are available at http://www.ou.edu/ieg/publications/datasets. Additional data files and r-scripts are available at https://osf.io/thjxs/. Community-weighted mean trait data are available as Supplementary Data 1–3.

Code availability

R-script used for data formatting and statistics are available on the Open Science Framework website https://osf.io/thjxs/. Code for the simulation is available as Supplementary Data 4.

Received: 9 June 2018; Accepted: 25 June 2019;
Published online: 19 August 2019

References

1. Grigulis, K. et al. Relative contributions of plant traits and soil microbial properties to mountain grassland ecosystem services. *J. Ecol.* **101**, 47–57 (2013).
2. Funk, J. L. et al. Revisiting the holy grail: using plant functional traits to understand ecological processes. *Biol. Rev. Camb. Phil. Soc.* **92**, 1156–1173 (2017).
3. Wardle, D. A. et al. Ecological linkages between aboveground and belowground biota. *Science* **304**, 1629–1633 (2004).
4. Bardgett, R. D. & van der Putten, W. H. Belowground biodiversity and ecosystem functioning. *Nature* **515**, 505–511 (2014).
5. Díaz, S. & Cabido, M. Vive la différence: plant functional diversity matters to ecosystem processes. *Trends Ecol. Evol.* **16**, 646–655 (2001).
6. Enquist, B. J. et al. Scaling from traits to ecosystems. *Adv. Ecol. Res.* **52**, 249–318 (2015).
7. Green, J. L., Bohannan, B. J. M. & Whitaker, R. J. Microbial biogeography: from taxonomy to traits. *Science* **320**, 1039–1043 (2008).
8. Martiny, A. C., Treseder, K. & Pusch, G. Phylogenetic conservatism of functional traits in microorganisms. *ISME J.* **7**, 830–838 (2013).
9. Bardgett, R. D., Mommer, L. & De Vries, F. T. Going underground: root traits as drivers of ecosystem processes. *Trends Ecol. Evol.* **29**, 692–699 (2014).
10. Krause, S. et al. Trait-based approaches for understanding microbial biodiversity and ecosystem functioning. *Front. Microbiol.* **5**, 251 (2014).
11. Martiny, J. B. H., Jones, S. E., Lennon, J. T. & Martiny, A. C. Microbiomes in light of traits: a phylogenetic perspective. *Science* **350**, aac9323 (2015).
12. Díaz, S. & Cabido, M. Plant functional types and ecosystem function in relation to global change. *J. Veg. Sci.* **8**, 463–474 (1997).
13. Kattge, J. et al. TRY–a global database of plant traits. *Glob. Change Biol.* **17**, 2905–2935 (2011).
14. Kimball, S. et al. Can functional traits predict plant community response to global change? *Ecosphere* **7**, e01602 (2016).
15. Enquist, B. J. et al. Assessing trait-based scaling theory in tropical forests spanning a broad temperature gradient. *Glob. Ecol. Biogeogr.* **26**, 1357–1373 (2017).
16. Lennon, J. T., Aanderud, Z. T., Lehmkuhl, B. K. & Schoolmaster, D. R. Mapping the niche space of soil microorganisms using taxonomy and traits. *Ecology* **93**, 1867–1879 (2012).
17. Edwards, K. F., Litchman, E. & Klausmeier, C. A. Functional traits explain phytoplankton community structure and seasonal dynamics in a marine ecosystem. *Ecol. Lett.* **16**, 56–63 (2013).
18. Pellissier, L. et al. Plant species distributions along environmental gradients: do belowground interactions with fungi matter? *Front. Plant Sci.* **4**, 500 (2013).
19. Phillips, R. P., Brzostek, E. & Midgley, M. G. The mycorrhizal-associated nutrient economy: a new framework for predicting carbon-nutrient couplings in temperate forests. *New Phytol.* **199**, 41–51 (2013).
20. Bennett, J. A. & Klironomos, J. Climate, but not trait, effects on plant-soil feedback depend on mycorrhizal type in temperate forests. *Ecosphere* **9**, e02132 (2018).
21. Barberán, A. et al. Relating belowground microbial composition to the taxonomic, phylogenetic, and functional trait distributions of trees in a tropical forest. *Ecol. Lett.* **18**, 1397–1405 (2015).
22. Reich, P. B. The world-wide 'fast–slow' plant economics spectrum: a traits manifesto. *J. Ecol.* **102**, 275–301 (2014).
23. Clarke, A. *Principles of Thermal Ecology: Temperature, Energy and Life* (Oxford Univ. Press, 2017).
24. Michaletz, S. T. et al. The energetic and carbon economic origins of leaf thermoregulation. *Nat. Plants* **2**, 16129 (2016).
25. Kobe, R. K., Lepczyk, C. A. & Iyer, M. Resorption efficiency decreases with increasing green leaf nutrients in a global dataset. *Ecology* **86**, 2780–2792 (2005).
26. Parton, W. et al. Global-scale similarities in nitrogen release patterns during long-term decomposition. *Science* **315**, 361–364 (2007).
27. Garnier, E. et al. Plant functional markers capture ecosystem properties during secondary succession. *Ecology* **85**, 2630–2637 (2004).
28. Reich, P. B. & Oleksyn, J. Global patterns of plant leaf N and P in relation to temperature and latitude. *Proc. Natl Acad. Sci. USA* **101**, 11001–11006 (2004).
29. Han, W., Fang, J., Guo, D. & Zhang, Y. Leaf nitrogen and phosphorus stoichiometry across 753 terrestrial plant species in China. *New Phytol.* **168**, 377–385 (2005).
30. He, M. et al. Leaf nitrogen and phosphorus of temperate desert plants in response to climate and soil nutrient availability. *Sci. Rep.* **4**, 6932 (2014).
31. Chapin, F. S. 3rd Effects of plant traits on ecosystem and regional processes: a conceptual framework for predicting the consequences of global change. *Ann. Bot.* **91**, 455–463 (2003).
32. Cornwell, W. K. et al. Plant species traits are the predominant control on litter decomposition rates within biomes worldwide. *Ecol. Lett.* **11**, 1065–1071 (2008).
33. Hobbie, S. E. Plant species effects on nutrient cycling: revisiting litter feedbacks. *Trends Ecol. Evol.* **30**, 357–363 (2015).
34. Bakker, M. A., Carreño-Rocabado, G. & Poorter, L. Leaf economics traits predict litter decomposition of tropical plants and differ among land use types. *Funct. Ecol.* **25**, 473–483 (2010).
35. Cheeke, T. E. et al. Dominant mycorrhizal association of trees alters carbon and nutrient cycling by selecting for microbial groups with distinct enzyme function. *New Phytol.* **214**, 432–442 (2017).
36. Averill, C., Dietze, M. C. & Bhatnagar, J. M. Continental-scale nitrogen pollution is shifting forest mycorrhizal associations and soil carbon stocks. *Glob. Chang. Biol.* **24**, 4544–4553 (2018).
37. Lambers, H., Poorter, H. & Van Vuuren, M. M. I. (eds) *Inherent Variation in Plant Growth: Physiological Mechanisms and Ecological Consequences* (Backhuys, 1998).
38. Read, D. J. & Perez-Moreno, J. Mycorrhizas and nutrient cycling in ecosystems—a journey towards relevance? *New Phytol.* **157**, 475–492 (2003).
39. Kerkhoff, A. J., Enquist, B. J., Elser, J. J. & Fagan, W. F. Plant allometry, stoichiometry and the temperature-dependence of primary productivity: plant allometry, stoichiometry and productivity. *Glob. Ecol. Biogeogr.* **14**, 585–598 (2005).

40. Walker, T. W. & Syers, J. K. The fate of phosphorus during pedogenesis. *Geoderma* **15**, 1–19 (1976).
41. Vitousek, P. M. & Farrington, H. Nutrient limitation and soil development: experimental test of a biogeochemical theory. *Biogeochemistry* **37**, 63–75 (1997).
42. Elser, J. J., Dobberfuhl, D. R., MacKay, N. A. & Schampel, J. H. Organism size, life history, and N:P stoichiometry. *Bioscience* **46**, 674–684 (1996).
43. Elser, J. J. et al. Biological stoichiometry from genes to ecosystems. *Ecol. Lett.* **3**, 540–550 (2000).
44. Elser, J. J. et al. Growth rate–stoichiometry couplings in diverse biota. *Ecol. Lett.* **6**, 936–943 (2003).
45. Levins, R. *Evolution in Changing Environments: Some Theoretical Explorations* (Princeton Univ. Press, 1968).
46. Carnicer, J. et al. A unified framework for diversity gradients: the adaptive trait continuum. *Glob. Ecol. Biogeogr.* **22**, 6–18 (2012).
47. Carnicer, J. et al. Global biodiversity, stoichiometry and ecosystem function responses to human-induced C–N–P imbalances. *J. Plant Physiol.* **172**, 82–91 (2015).
48. Hartman, W. H. & Richardson, C. J. Differential nutrient limitation of soil microbial biomass and metabolic quotients (qCO_2): is there a biological stoichiometry of soil microbes? *PLoS ONE* **8**, e57127 (2013).
49. Grace, J. B. et al. Guidelines for a graph-theoretic implementation of structural equation modeling. *Ecosphere* **3**, 73 (2012).
50. Lefcheck, J. S. piecewiseSEM : piecewise structural equation modelling in r for ecology. *Methods Ecol. Evol.* **7**, 573–579 (2016).
51. Shipley, B. The AIC model selection method applied to path analytic models compared using a d-separation test. *Ecology* **94**, 560–564 (2013).
52. Reich, P. B. et al. Generality of leaf trait relationships: a test across six biomes. *Ecology* **80**, 1955–1969 (1999).
53. Craine, J. M. et al. Global patterns of foliar nitrogen isotopes and their relationships with climate, mycorrhizal fungi, foliar nutrient concentrations, and nitrogen availability. *New Phytol.* **183**, 980–992 (2009).
54. Koerselman, W. & Meuleman, A. F. M. The vegetation N:P ratio: a new tool to detect the nature of nutrient limitation. *J. Appl. Ecol.* **33**, 1441–1450 (1996).
55. Craine, J. M. et al. Convergence of soil nitrogen isotopes across global climate gradients. *Sci. Rep.* **5**, 8280 (2015).
56. Chalot, M. & Brun, A. Physiology of organic nitrogen acquisition by ectomycorrhizal fungi and ectomycorrhizas. *FEMS Microbiol. Rev.* **22**, 21–44 (1998).
57. Enquist, B. J. & Niklas, K. J. Invariant scaling relations across tree-dominated communities. *Nature* **410**, 655–660 (2001).
58. Zhou, J. et al. Temperature mediates continental-scale diversity of microbes in forest soils. *Nat. Commun.* **7**, 12083 (2016).
59. Weiser, M. D. et al. Toward a theory for diversity gradients: the abundance-adaptation hypothesis. *Ecography* **41**, 255–264 (2018).
60. Westoby, M. A leaf–height–seed (LHS) plant ecology strategy scheme. *Plant Soil* **199**, 213–227 (1998).
61. Wright, I. J. et al. The worldwide leaf economics spectrum. *Nature* **428**, 821–827 (2004).
62. Van Der Heijden, M. G. A. & Scheublin, T. R. Functional traits in mycorrhizal ecology: their use for predicting the impact of arbuscular mycorrhizal fungal communities on plant growth and ecosystem functioning. *New Phytol.* **174**, 244–250 (2007).
63. Legay, N. et al. Influence of plant traits, soil microbial properties, and abiotic parameters on nitrogen turnover of grassland ecosystems. *Ecosphere* **7**, e01448 (2016).
64. Eviner, V. T., Chapin, F. S. 3rd & Vaughn, C. E. Seasonal variations in plant species effects on soil N and P dynamics. *Ecology* **87**, 974–986 (2006).
65. Violle, C., Reich, P. B., Pacala, S. W., Enquist, B. J. & Kattge, J. The emergence and promise of functional biogeography. *Proc. Natl Acad. Sci. USA* **111**, 13690–13696 (2014).
66. Hevia, V. et al. Trait-based approaches to analyze links between the drivers of change and ecosystem services: synthesizing existing evidence and future challenges. *Ecol. Evol.* **7**, 831–844 (2017).
67. Zhou, J. et al. Reproducibility and quantitation of amplicon sequencing-based detection. *ISME J.* **5**, 1303–1313 (2011).
68. Zhou, J. et al. Random sampling process leads to overestimation of β-iversity of microbial communities. *MBio* **4**, e00324–13 (2013).
69. Zhou, J. et al. High-throughput metagenomic technologies for complex microbial community analysis: open and closed formats. *MBio* **6**, e02288–14 (2015).
70. Lear, G. et al. Methods for the extraction, storage, amplification and sequencing of DNA from environmental samples. *N. Z. J. Ecol.* **42**, 10–50A (2018).
71. Pérez-Harguindeguy, N. et al. New handbook for standardised measurement of plant functional traits worldwide. *Aust. J. Bot.* **61**, 167–234 (2013).
72. Reich, P. B., Walters, M. B. & Ellsworth, D. S. From tropics to tundra: global convergence in plant functioning. *Proc. Natl Acad. Sci. USA* **94**, 13730–13734 (1997).
73. Poorter, H. & Lambers, H. Is interspecific variation in relative growth rate positively correlated with biomass allocation to the leaves? *Am. Nat.* **138**, 1264–1268 (1991).
74. Hodgson, J. G. et al. Is leaf dry matter content a better predictor of soil fertility than specific leaf area? *Ann. Bot.* **108**, 1337–1345 (2011).
75. Robinson, D. δ^{15}N as an integrator of the nitrogen cycle. *Trends Ecol. Evol.* **16**, 153–162 (2001).
76. Hobbie, E. A. & Colpaert, J. V. Nitrogen availability and colonization by mycorrhizal fungi correlate with nitrogen isotope patterns in plants. *New Phytol.* **157**, 115–126 (2003).
77. Kerkhoff, A. J., Enquist, B. J., Elser, J. J. & Fagan, W. F. Plant allometry, stoichiometry and the temperature-dependence of primary productivity. *Glob. Ecol. Biogeogr.* **14**, 585–598 (2005).
78. Gloaguen, J. C. & Touffet, J. C–N evolution in the leaves and during litter decomposition under Atlantic climate—the beech and some conifers. *Ann. Des. Sci. For.* **39**, 219–230 (1982).
79. Enríquez, S., Duarte, C. M. & Sand-Jensen, K. Patterns in decomposition rates among photosynthetic organisms: the importance of detritus C:N:P content. *Oecologia* **94**, 457–471 (1993).
80. Pérez-Harguindeguy, N. et al. Chemistry and toughness predict leaf litter decomposition rates over a wide spectrum of functional types and taxa in central Argentina. *Plant Soil* **218**, 21–30 (2000).
81. Zhou, J., Bruns, M. A. & Tiedje, J. M. DNA recovery from soils of diverse composition. *Appl. Environ. Microbiol.* **62**, 316–322 (1996).
82. Magoč, T. & Salzberg, S. L. FLASH: fast length adjustment of short reads to improve genome assemblies. *Bioinformatics* **27**, 2957–2963 (2011).
83. Kong, Y. Btrim: a fast, lightweight adapter and quality trimming program for next-generation sequencing technologies. *Genomics* **98**, 152–153 (2011).
84. Edgar, R. C., Haas, B. J., Clemente, J. C., Quince, C. & Knight, R. UCHIME improves sensitivity and speed of chimera detection. *Bioinformatics* **27**, 2194–2200 (2011).
85. Edgar, R. C. Search and clustering orders of magnitude faster than BLAST. *Bioinformatics* **26**, 2460–2461 (2010).
86. DeSantis, T. Z. et al. Greengenes, a chimera-checked 16S rRNA gene database and workbench compatible with ARB. *Appl. Environ. Microbiol.* **72**, 5069–5072 (2006).
87. Caporaso, J. G. et al. PyNAST: a flexible tool for aligning sequences to a template alignment. *Bioinformatics* **26**, 266–267 (2010).
88. Edgar, R. C. MUSCLE: multiple sequence alignment with high accuracy and high throughput. *Nucleic Acids Res.* **32**, 1792–1797 (2004).
89. Price, M. N., Dehal, P. S. & Arkin, A. P. FastTree 2—approximately maximum-likelihood trees for large alignments. *PLoS ONE* **5**, e9490 (2010).
90. Wang, Q., Garrity, G. M., Tiedje, J. M. & Cole, J. R. Naive Bayesian classifier for rapid assignment of rRNA sequences into the new bacterial taxonomy. *Appl. Environ. Microbiol.* **73**, 5261–5267 (2007).
91. McMurdie, P. J. & Holmes, S. Waste not, want not: why rarefying microbiome data is inadmissible. *PLoS Comput. Biol.* **10**, e1003531 (2014).
92. Gloor, G. B., Macklaim, J. M., Pawlowsky-Glahn, V. & Egozcue, J. J. Microbiome datasets are compositional: and this is not optional. *Front. Microbiol.* **8**, 2224 (2017).
93. Tu, Q. et al. GeoChip 4: a functional gene-array-based high-throughput environmental technology for microbial community analysis. *Mol. Ecol. Resour.* **14**, 914–928 (2014).
94. Wang, C. et al. Aridity threshold in controlling ecosystem nitrogen cycling in arid and semi-arid grasslands. *Nat. Commun.* **5**, 4799 (2014).
95. Nguyen, N. H. et al. FUNGuild: an open annotation tool for parsing fungal community datasets by ecological guild. *Fungal Ecol.* **20**, 241–248 (2016).
96. Wang, B. & Qiu, Y.-L. Phylogenetic distribution and evolution of mycorrhizas in land plants. *Mycorrhiza* **16**, 299–363 (2006).
97. He, Z. et al. GeoChip 3.0 as a high-throughput tool for analyzing microbial community composition, structure and functional activity. *ISME J.* **4**, 1167–1179 (2010).
98. He, Z. et al. GeoChip: a comprehensive microarray for investigating biogeochemical, ecological and environmental processes. *ISME J.* **1**, 67–77 (2007).
99. Wen, C. et al. Evaluation of the reproducibility of amplicon sequencing with Illumina MiSeq platform. *PLoS ONE* **12**, e0176716 (2017).
100. Groemping, U. Relative importance for linear regression in R: the package relaimpo. *J. Stat. Softw.* **17**, 1–27 (2006).

Acknowledgements

We thank the members of the LTER Network and the Smithsonian Tropical Research Institute—Barro Colorado Island who participated in data collection. We thank C. Sides, T. Birt, L. Sloat, A. Henderson, J. Messier and B. Blonder for field assistance with vegetation sampling. We thank J. Wright for assistance with sampling at Barro Colorado

Island. We also thank E. Brodie for helpful comments on earlier drafts. Funding for this study was provided by the US National Science Foundation MacroSystems Biology program NSF EF-1065844.

Author contributions

All authors contributed to the intellectual development of this study. V.B., B.J.E., M.K., S.T.M. and M.D.W. collected the field experimental data. Y.D., Z.H., J.Z., D.N., L.S., Q.T., J.V. and J.W. collected the sequencing and GeoChip data, and performed statistical analyses and data integration for microbial communities. D.N. developed and ran the simulation comparing rarefied versus non-rarefied sequence data. V.B., B.J.E. and S.T.M. performed statistical analyses and drafted the manuscript with help from Z.H., J.Z., M.K., R.W. and M.D.W.

Competing interest

The authors declare no competing interests.

Additional information

Supplementary information is available for this paper at https://doi.org/10.1038/s41559-019-0954-7.

Reprints and permissions information is available at www.nature.com/reprints.

Correspondence and requests for materials should be addressed to V.B.

Publisher's note: Springer Nature remains neutral with regard to jurisdictional claims in published maps and institutional affiliations.

nature research

Corresponding author(s): Vanessa Buzzard and Brian J. Enquist

Last updated by author(s): Jun 18, 2019

Reporting Summary

Nature Research wishes to improve the reproducibility of the work that we publish. This form provides structure for consistency and transparency in reporting. For further information on Nature Research policies, see Authors & Referees and the Editorial Policy Checklist.

Statistics

For all statistical analyses, confirm that the following items are present in the figure legend, table legend, main text, or Methods section.

n/a	Confirmed
☐	☒ The exact sample size (*n*) for each experimental group/condition, given as a discrete number and unit of measurement
☐	☒ A statement on whether measurements were taken from distinct samples or whether the same sample was measured repeatedly
☐	☒ The statistical test(s) used AND whether they are one- or two-sided *Only common tests should be described solely by name; describe more complex techniques in the Methods section.*
☐	☒ A description of all covariates tested
☐	☒ A description of any assumptions or corrections, such as tests of normality and adjustment for multiple comparisons
☐	☒ A full description of the statistical parameters including central tendency (e.g. means) or other basic estimates (e.g. regression coefficient) AND variation (e.g. standard deviation) or associated estimates of uncertainty (e.g. confidence intervals)
☐	☒ For null hypothesis testing, the test statistic (e.g. *F*, *t*, *r*) with confidence intervals, effect sizes, degrees of freedom and *P* value noted *Give P values as exact values whenever suitable.*
☒	☐ For Bayesian analysis, information on the choice of priors and Markov chain Monte Carlo settings
☒	☐ For hierarchical and complex designs, identification of the appropriate level for tests and full reporting of outcomes
☒	☐ Estimates of effect sizes (e.g. Cohen's *d*, Pearson's *r*), indicating how they were calculated

Our web collection on statistics for biologists contains articles on many of the points above.

Software and code

Policy information about availability of computer code

Data collection	Trait data for the most abundant tree species based on basal area were collected for 30- 0.1 Ha forest plots. PCR amplicons for soil microbes were sequenced using Illumina MySeq. Functional genes for soil microbes were determine using a functional gene microarray, GeoChip 5.0.
Data analysis	All final data analyses, statistics, and figures were conducted using R (Version 3.3.1, https://www.R-project.org/). Details on GeoChip 5.0 hybridization can be found at http://ieg.ou.edu/protocol.htm. Algorithms and software used for sequencing include the following software: Chimera Slayer, FLASH, UCLUST, BLAST, PyNAST, FastTree, and RDP classifier.

For manuscripts utilizing custom algorithms or software that are central to the research but not yet described in published literature, software must be made available to editors/reviewers. We strongly encourage code deposition in a community repository (e.g. GitHub). See the Nature Research guidelines for submitting code & software for further information.

Data

Policy information about availability of data

All manuscripts must include a data availability statement. This statement should provide the following information, where applicable:

- Accession codes, unique identifiers, or web links for publicly available datasets
- A list of figures that have associated raw data
- A description of any restrictions on data availability

Data Availability
Raw sequencing data have been deposited in the NCBI Sequence Read Archive under accession code PRJNA308872. The OTU tables and microarray data presented are available at http://www.ou.edu/ieg/publications/datasets. Additional data files and r-scripts are available at https://osf.io/thjxs/. Community weighted mean trait data are available as Supplementary Data File 1-3.
Code Availability
R-script used for data formatting and statistics are available on the Open Science Framework website https://osf.io/thjxs/. Code for the simulation is available as

Supplementary Data File 4.

Field-specific reporting

Please select the one below that is the best fit for your research. If you are not sure, read the appropriate sections before making your selection.

☐ Life sciences ☐ Behavioural & social sciences ☒ Ecological, evolutionary & environmental sciences

For a reference copy of the document with all sections, see nature.com/documents/nr-reporting-summary-flat.pdf

Ecological, evolutionary & environmental sciences study design

All studies must disclose on these points even when the disclosure is negative.

Study description	This study includes 30 0.1 hectare forest plots and 126 1 meter-squared soil plots across six sites. All tree species above 1cm diameter at ground height were measured and identified. Traits were collected from the 5 most abundant species based on basal area for each plot. Nine soil-surface cores (10cm depth) were collected and homogenized for each soil plot and DNA was extracted from 5 grams of soil for which Illumina MySeq and GeoChip microarray were run. One HOBO Micro Station (Part # H21-002) was installed in each of the five Gentry tree plots at all six experimental sites to monitor continuous variation in soil moisture (using Soil Moisture Smart Sensor Part # S-SMB-M005) and temperature (12-Bit Temperature Smart Sensor Part # S-TMB-M002).
Research sample	Research samples comprised all plants above 1cm at ground height that are rooted within six 500 x 2m Gentry style plots and nine homogenized soil core samples from 126 1 x 1m soil plots. The number of individuals and species varied widely between sites. The sites chosen represent a broad gradient in temperature and latitude of relatively undisturbed forests.
Sampling strategy	All tree and soil plots are located within a 25 Hectare plot to capture spatial variation at each of the 6 study sites. Community weighted means were used to to assess trait variation of the most dominant species.
Data collection	Data were collected by authors.
Timing and spatial scale	All samples were collected during peak growing season during 2012 and 2013.
Data exclusions	To be consistent with methods used for microbial analyses, observations for multiple species within each genus were averaged to create a genus-level mean trait value for each plot. This only occurred when multiple measurements per species per genus were available. Chloroplast, mitochondria and archaeal sequences were removed. In addition, singletons detected solely in one of the subsamples were discarded prior to the statistical analyses to 85 remove noise from the data set.
Reproducibility	Species identification was conducted by local botanists at each site and species vouchers were deposited in local herbaria. Detailed protocols for soil DNA extraction, amplification and sequencing can be found on the IEG website (http://ieg.ou.edu/protocol.htm.).
Randomization	All sites were randomly located and plots within each site were systematically placed within the 25 Hectare area as to maintain consistency between sites and reduce plots selection.
Blinding	N/A

Did the study involve field work? ☒ Yes ☐ No

Field work, collection and transport

Field conditions	All fieldwork occurred during peak growing season at each site and more detailed information is available on http://macroeco.lternet.edu/.
Location	Location information is available in the extended data figures and http://macroeco.lternet.edu/. HJ Andrews LTER: Coniferous Forest, Longitude: -122.151041, Latitude: 44.231094, Elevation (m): 860, Mean Annual Temperature (C): 8.5, Mean Annual Precipitation (mm): 2200. Coweeta LTER: Deciduous Forest, Longitude: -83.431501, Latitude: 35.048415, Elevation (m): 864, Mean Annual Temperature (C): 13.3, Mean Annual Precipitation (mm): 1906. Harvard Forest LTER: Deciduous Forest, Longitude: -72.177094, Latitude: 42.539036, Elevation (m) 356.4, Mean Annual Temperature (C): 7.1, Mean Annual Precipitation (mm): 1066. Luquillo LTER: Tropical Rainforest, Longitude: -65.815575, Latitude: 18.324278, Elevation (m) 385.8, Mean Annual Temperature (C): 22.8, Mean Annual Precipitation (mm): 3460. Niwot Ridge: LTER Alpine Tundra, Longitude: -105.558347, Latitude: 40.040896, Elevation (m) 3186, Mean Annual Temperature (C): -3.2, Mean Annual Precipitation (mm): 930. Barro Colorado Island: Tropical Rainforest, Longitude: -79.845988, Latitude: 9.15872, Elevation (m) 157.1, Mean Annual Temperature (C): 27.5, Mean Annual Precipitation (mm): 2623.
Access and import/export	Our sample processing and collection followed all applicable laws and used all necessary export and import permits.
Disturbance	None.

Reporting for specific materials, systems and methods

We require information from authors about some types of materials, experimental systems and methods used in many studies. Here, indicate whether each material, system or method listed is relevant to your study. If you are not sure if a list item applies to your research, read the appropriate section before selecting a response.

Materials & experimental systems

n/a	Involved in the study
☒	☐ Antibodies
☒	☐ Eukaryotic cell lines
☒	☐ Palaeontology
☒	☐ Animals and other organisms
☒	☐ Human research participants
☒	☐ Clinical data

Methods

n/a	Involved in the study
☒	☐ ChIP-seq
☒	☐ Flow cytometry
☒	☐ MRI-based neuroimaging